



## Two-Dimensional Magnetized Mixed Convection Hybrid Nanofluid Over a Vertical Exponentially Shrinking Sheet by Thermal Radiation, Joule Heating, Velocity and Thermal Slip Conditions

Adnan Asghar<sup>1</sup>, Teh Yuan Ying<sup>1,\*</sup>, Khairy Zaimi<sup>2</sup>

<sup>1</sup> School of Quantitative Sciences, UUM College of Arts & Sciences, Universiti Utara Malaysia, 06010 UUM Sintok, Kedah Darul Aman, Malaysia

<sup>2</sup> Faculty of Applied and Human Sciences, Universiti Malaysia Perlis, Jalan Kangar-Alor Setar, Pengkalan Asam, 01000 Kangar, Perlis, Malaysia

### ARTICLE INFO

#### Article history:

Received 19 February 2022

Received in revised form 30 April 2022

Accepted 3 May 2022

Available online 2 June 2022

#### Keywords:

Hybrid nanofluid; boundary layer; mixed convection; MHD; radiation; Joule heating; velocity slip; thermal slip

### ABSTRACT

Hybrid nanofluid is an improved kind of nanofluid that typically utilized to enhance the thermal efficiency in fluid flow regimes. It has a wide range of real-world applications. This opened up many new prospects to further investigate the two-dimensional hybrid nanofluid under different body geometries and physical parameters. A numerical study of a two-dimensional magnetized mixed convection hybrid nanofluid flow over a vertical exponentially shrinking sheet is considered in this paper. The main objective of this current study is to examine the influences of volume fraction of copper, mixed convection, and radiation on the reduced skin friction and reduced heat transfer against the effect of suction. Besides, the influences of radiation, volume fraction of alumina, velocity slip, thermal slip, magnetic parameter, and Eckert number on the velocity and temperature profiles are also considered in this paper. The governing system of partial differential equations (PDEs) is transformed into a system of nonlinear ordinary differential equations (ODEs) through exponential similarity variables. Then, the `bvp4c` solver for MATLAB is used to solve the transformed nonlinear ODEs. Numerous significant results are being observed. As the quantity of mixed convection was raised, the reduced skin friction improved in both solutions, and reduced heat transfer increased in the second solution but with no variation found in the first solution. Besides, the temperature profile grew when the volume fraction of alumina, radiation, magnetic parameter, and Eckert number were raised in both solutions. In terms of heat transfer rate, when the amount of the velocity slip parameter was increased, temperature reduced in the first solution but increased in the second solution. Whilst temperature dropped in both solutions as the thermal slip parameter was enhanced. In conclusion, the addition of hybrid nanoparticles boosted the heat transmission rate. In the assisting flow condition, dual solutions exist when the suction parameter value is greater or equal to its critical point. However, no fluid flow is conceivable when the indicated value is less than this critical point.

\* Corresponding author.

E-mail address: [yuanying@uum.edu.my](mailto:yuanying@uum.edu.my)

<https://doi.org/10.37934/arfmts.95.2.159179>

## 1. Introduction

In the engineering and manufacturing industries, boundary layer flow generated through stretching or shrinking surface is usually employed. The notion of a two-dimensional boundary layer steady flow over a stretching surface was first explored by Sakiadis [1]. Subsequently, Crane [2] who had modified Sakiadis' concepts and applied them to two-dimensional linear stretching and exponential surfaces in a steady flow. For the previous few decades, scientists have focused their efforts on improving the heat transfer rate in industrial and engineering applications. This is due to the fact that the performances of many devices such as electronic devices and heat exchangers, are highly dependent on the heat transfer rate. Normal fluids such as oil, ethylene glycol, and water have limited heat transfer rate due to their low thermal conductivity. In view this, the aforementioned normal fluids' deficiencies could be solved by incorporating a single or more than one type of nanoparticles into the normal fluids.

Choi and Eastman [3] was the first to describe such combination of nanoparticles and normal fluids as nanofluids. Nanofluids are composed of tiny quantities of solid particles measuring 100 nm or less in size. Solid nanoparticles have the ability to significantly upsurge the thermal conductivity and heat transfer rate of normal fluids. Metals (such as iron (Fe), aluminium (Al), copper (Cu)), metal oxides (such as copper (II) oxide (CuO), alumina (Al<sub>2</sub>O<sub>3</sub>)), and semiconductors (such as titanium dioxide (TiO<sub>2</sub>), silicon dioxide (SiO<sub>2</sub>)) are among those common nanoparticles being explored by many researchers in the existing literature. Known applications which involved nanofluids exist in the fields of solar energy, drug delivery, aircraft, agriculture, building cooling and heating, microchips, refrigerators, and vehicles [4]. Miklavčič and Wang [5] were acknowledged as being the first to employ suction to examine the viscosity of three-dimensional fluid flow across a shrinking surface. Moreover, Qayyum *et al.*, [6] investigated the influences of copper and silver nanoparticles on the two-dimensional flow of homogeneous-heterogeneous processes in the occurrence of radiation. Ahmad and Pop [7] explored the notion of two-dimensional mixed convection steady flow on nanofluid and concluded that non-uniqueness of solutions exists only within certain parameter regions. Entropy generation minimization (EGM) of two-dimensional radiative nanofluid flow through a thin moving needle was studied by Khan *et al.*, [8]. The two-dimensional flow across an exponentially stretched surface was studied by Magyari and Keller [9], and Elbashbeshy [10] followed up with a similar investigation which considered the mass suction on the exponentially surface. More recent studies of nanofluid at various physical parameters can be seen in the existing literature [11-22].

On the other hand, hybrid nanofluid is a new type of nanofluid with a composition of more than one distinct type nanoparticles in a normal fluid. Such composition further improves the thermal characteristics exhibited by nanofluid. Paper production, air conditioning systems, warmth pipes, tube-shaped heat exchangers, helical coil heat exchangers, and other uses of hybrid nanofluids were described by Huminic and Huminic [23]. Suresh *et al.*, [24] developed the concept of hybrid nanofluids through laboratory experiment. Devi and Devi [25] explored a two-dimensional boundary layer MHD steady flow of Al<sub>2</sub>O<sub>3</sub>-Cu/H<sub>2</sub>O hybrid nanofluid across a stretched surface employing novel thermophysical characteristic correlations which agreed with the findings of Suresh *et al.*, [24]. They revealed that greater nanoparticle volume fractions would increase heat transfer rate in those investigations. Waini *et al.*, [26] focused on a two-dimensional unsteady flow and heat transfer via a stretching/shrinking layer in a hybrid nanofluid. Besides, the heat transfer of a steady two-dimensional hybrid nanofluid over an exponentially stretching/shrinking layer was investigated by Yashkun *et al.*, [27] through the impact of Joule heating and mixed convection. Zainal *et al.*, [28] examined the influence of heat generation/absorption on a three-dimensional MHD steady flow of

an  $\text{Al}_2\text{O}_3\text{-Cu}/\text{H}_2\text{O}$  hybrid nanofluid over a bidirectional exponential stretching/shrinking layer. According to the findings by Yashkun *et al.*, [27] and Zainal *et al.*, [28], the heat transfer rate increased when the volume fraction nanoparticles is enhanced. Several reviews and findings on exponentially hybrid nanofluids can be found in the literature [29-32].

Magnetohydrodynamics (MHD) is a term that combines the words magneto (magnetic), hydro (fluids), and dynamics (motion). MHD is the study of electrically conducting fluid flow under the influence of magnetic field. Engineers employed MHD ideas in developing and designing a wide range of industrial applications, including generators, MHD pumps, flow meters, nuclear waste disposal, geothermal energy extractors, nuclear reactor cooling, and others [33]. Devi and Devi [34] expanded their findings in Devi and Devi [25] to a three-dimensional steady flow employing Newtonian heating. They revealed that hybrid nanofluid transfers heat more rapidly than nanofluid. Besides, a steady two-dimensional flow of a hybrid nanofluid across a stretching layer was then explored by Devi and Devi [35]. Lund *et al.*, [36] investigated a two-dimensional unsteady MHD hybrid nanofluid flow over a stretching and shrinking sheet with the effect of radiation. Waini *et al.*, [37] investigated the impact of radiation on a two-dimensional steady MHD hybrid nanofluid flow passes through an exponentially shrinking layer. Additional studies on MHD hybrid nanofluid were included in the references [38,39].

At high operating temperatures, thermal radiation has a considerable influence that must be taken into account. Thermal radiation sensitivity is crucial in designing a suitable apparatus since many industrial processes occur at extremely high temperatures. Solar radiations, ship compressors, internal combustion engines, spaceships, combustion processes, plasma physics, and spacecraft are among the many industrial applications in which it is used [40]. Sreedevi *et al.*, [41] used radiation to study its impact on a two-dimensional unsteady hybrid nanofluid flow of mass and heat across a stretched sheet. Hayat and Nadeem [42] explored the heat transfer of a three-dimensional steady flow employing an  $\text{Ag-CuO}/\text{water}$  hybrid nanofluid. Anuar *et al.*, [43] explained a three-dimensional steady rotating hybrid nanofluid flow over a stretching and shrinking sheet through radiation parameter. Recently, Dero *et al.*, [44] examined the numerical analysis of a  $\text{Cu-Al}_2\text{O}_3/\text{H}_2\text{O}$  hybrid nanofluid of cross and streamwise flows under the influence of thermal radiation. More researches have been conducted on hybrid nanofluid in the occurrence of thermal radiation [45,46].

Convective heat transfer, commonly known as convection, is a heat transfer process from one location to another through a moving heated fluid flow. Forced convection is the procedure in which flow pattern is created by an external source. Free or natural convection is a mechanism in which flow pattern is driven only by buoyant forces caused by density fluctuations. Mixed convection exists when both forced and natural convection processes are involved [47]. Due to its significance effect in solar collectors, nuclear reactors, vehicle radiators, and electronic devices, the phenomenon of mixed convection flow has piqued the interest of researchers [48]. Merkin [49] was the first to explore a two-dimensional mixed convection on boundary layer porous medium in the presence of multiple solutions. Later, in 1986, he continued his research on porous media and identified dual solutions [50]. Furthermore, Waini *et al.*, [51] investigated a two-dimensional steady hybrid nanofluid flow along a vertical plate in a porous media utilizing mixed convection. Additionally, Yashkun *et al.*, [27] explored a two-dimensional steady hybrid nanofluid flow by an exponentially stretching/shrinking layer, with the impact of mixed convection and Joule heating. However, they did not study the impact of the mixed convection parameter. Moreover, Waini *et al.*, [48] considered a two-dimensional steady flow across a vertical exponential stretching and shrinking surface in hybrid nanofluid with the occurrence of mixed convection. Mixed convection investigations have been studied by several other researchers [52,53].

The technique of creating heat by carrying an electric current via a conductor is known as Joule heating, also being characterized as ohmic, resistance, or resistive heating. Joule heating can be seen

in the resistance ovens, incandescent light bulbs, cartridge heaters, electric warmers, electric fuses, soldering irons, and food processing equipment [27]. Khashi'ie *et al.*, [54] also explored the behaviour of a steady two-dimensional MHD Cu-Al<sub>2</sub>O<sub>3</sub>/water nanofluid coupled with a radially stretching/shrinking sheet under the influence of Joule heating. Moreover, Yan *et al.*, [55] investigated a two-dimensional magnetized steady hybrid nanofluid flow by an exponential surface with the existence of Joule heating and slip conditions. Besides, they also discovered that increasing the Eckert number raises the temperature in both solutions.

Many significant applications of slip condition include the formation of heart valves and interior cavities, as well as the cleaning of artificial heart valves [56]. Andersson [57] was the first to propose the concept of slip influence on boundary flow. Hayat *et al.*, [58] investigated a three-dimensional rotating steady hybrid nanofluid flow with partial slip and radiation effect. Additionally, Yan *et al.*, [55], as mentioned above, investigated a two-dimensional magnetized steady hybrid nanofluid flow by an exponential surface with the presence of slip conditions and Joule heating. They noted that reduced heat transfer declines as in thermal slip parameter rises. More citations on the influence of slip parameter are presented in the literature [59,60].

Yashkun *et al.*, [27] studied a two-dimensional hybrid nanofluid flow including an exponentially stretching/shrinking sheet under the influence of MHD, Joule heating, and mixed convection, but without considering the effect of velocity and thermal slip conditions, as well as thermal radiation. Waini *et al.*, [48] explored a two-dimensional hybrid nanofluid flow across a vertical exponentially shrinking sheet using mixed convection without taking into account the effect of MHD, velocity and thermal slip conditions, Joule heating, and radiation. However, by using the Tiwari-Das model (see Tiwari and Das [61]), the present study aims to fill in the gaps reported in Yashkun *et al.*, [27] and Waini *et al.*, [48] by addressing the combined effect of MHD, mixed convection, radiation, Joule heating, as well as velocity and thermal slips conditions. Therefore, a novel physical model of two-dimensional magnetized mixed convection hybrid nanofluid over a vertical exponentially shrinking sheet with the effect of thermal radiation, Joule heating, velocity and thermal slip conditions has been developed. In this study, the hybrid nanofluid being considered is a composition of alumina (Al<sub>2</sub>O<sub>3</sub>) and copper (Cu) as the solid nanoparticles, and water (H<sub>2</sub>O) as the base fluid. The research aims to explore the variation influence of volume fraction of copper, mixed convection and thermal radiation on reduced skin friction and reduced heat transfer against the suction effect. Moreover, the velocity and temperature profiles with respect to radiation, the volume fraction of alumina, velocity and thermal slip conditions, MHD, and Eckert number are also being examined and discussed. Additionally, numerical findings from the current study are compared with those findings found in previous studies. To the best of the authors' knowledge, the findings of this study are novel and have yet to be examined and reported by any researcher.

## 2. Methodology

### 2.1 Formulation of Mathematical Modelling

The two-dimensional MHD mixed convection incompressible and steady flow on a vertical exponentially shrinking sheet in hybrid nanofluid is presented in Figure 1. The sheet movement is determined by the  $x$ -axis, whereas the  $y$ -axis is perpendicular to it. Along this  $x$ -axis, the surface velocity is  $u = u_w(x) = U_w e^{x/l}$ , where  $l$  is the characteristic length while  $U_w$  is a constant of the sheet. Moreover,  $T_w(x) = T_0 e^{2x/l} + T_\infty$ , where  $T_w(x)$  is the surface's temperature,  $T_\infty$  is the free stream temperature and  $T_0$  being the characteristic temperature.

The following assumptions were also applied in this physical model.

- i. In the physical model, both the heated plate ( $T_w(x) > T_\infty$ ) and cooled plate ( $T_w(x) < T_\infty$ ) are taken into consideration.
- ii. A magnetic field with varying strength is being applied in the direction parallel to the  $y$ -axis and being defined as  $B(x) = B_0 e^{x/2l}$  in which  $B_0$  denotes the magnetic field's constant intensity.
- iii. The symbol  $g$  represents the gravitational acceleration.

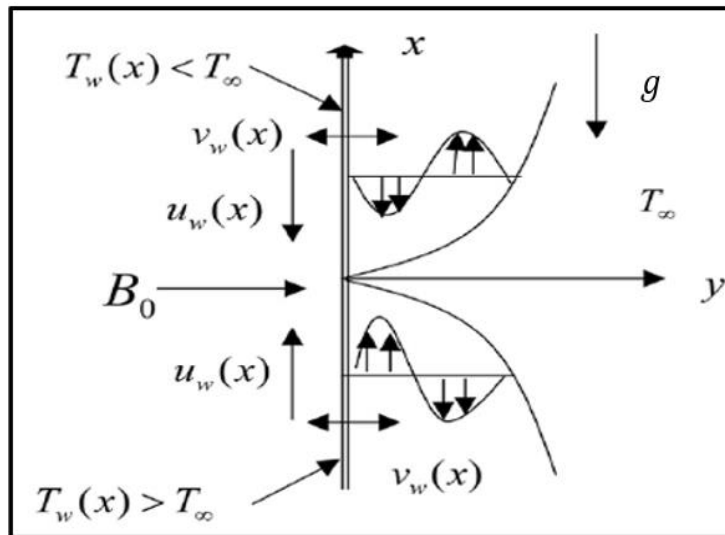


Fig. 1. The physical model considered in this study

The following are the governing equations for the abovementioned physical model [37,48,55]

$$u_x + v_y = 0, \tag{1}$$

$$uu_x + vu_y = \frac{\mu_{hnf}}{\rho_{hnf}} u_{yy} + \beta_{hnf} g(T - T_\infty) - \frac{\sigma_{hnf}}{\rho_{hnf}} B^2 u, \tag{2}$$

$$uT_x + vT_y = \frac{k_{hnf}}{(\rho c_p)_{hnf}} T_{yy} - \frac{1}{(\rho c_p)_{hnf}} (q_r)_y + \frac{\sigma_{hnf}}{(\rho c_p)_{hnf}} B^2 u^2 \tag{3}$$

The boundary conditions are as follows [55]:

$$v = v_w(x), u = u_w + \zeta v_f u_y, T = T_w + \xi v_f T_y \text{ as } y = 0, \tag{4}$$

$$u \rightarrow 0, T \rightarrow T_\infty, \text{ as } y \rightarrow \infty. \tag{5}$$

The variables  $u$  and  $v$  correspond to the velocities along the  $x$ - and  $y$ -axes, respectively.  $T$  is defined as the fluid's temperature. Furthermore,  $\zeta = \zeta_1 e^{-x/2l}$  is the velocity slip factor, and  $\zeta_1$  symbolizes the initial values of the velocity factor. On the other hand,  $\xi = \xi_1 e^{-x/2l}$  is the factor of thermal slip, and  $\xi_1$  signifies the initial values of the thermal factor. Besides,  $v_w = -(U_w v_f / 2l)^{1/2} e^{x/2l} S$  denotes the mass flux velocity where  $S$  is the parameter of suction/injection, with  $S > 0$  indicating suction and  $S < 0$  showing injection. The radiative heat flux is  $q_r$  [37]:

$$q_r = -\frac{4\sigma_1}{3k^1} \frac{\partial T^4}{\partial y}. \tag{6}$$

The Stefan-Boltzmann constant and the mean absorption coefficient are denoted by the symbols  $\sigma_1$  and  $k^1$ , respectively. By excluding higher-order terms and expanding  $T^4$  with a Taylor series about  $T_\infty$ , these yields  $T^4 \cong 4T_\infty^3 T - 3T_\infty^4$ , and readily to be substituted in Eq. (3) as follows [37]

$$uT_x + vT_y = \left[ \frac{k_{hnf}}{(\rho c_p)_{hnf}} + \frac{16\sigma_1 T_\infty^3}{3k^1(\rho c_p)_{hnf}} \right] T_{yy} + \frac{\sigma_{hnf}}{(\rho c_p)_{hnf}} B^2 u^2. \tag{7}$$

Besides,  $\sigma$ ,  $\beta$ ,  $\rho$ ,  $k$ ,  $c_p$ ,  $\rho c_p$ , and  $\mu$  are constants which represent the electrical conductivity, thermal expansion coefficient, density, thermal conductivity, specific heat capacity, effective heat capacity, and dynamic viscosity, respectively. The subscripts  $f$ ,  $nf$ ,  $hnf$ ,  $Al_2O_3$ , and  $Cu$  signify fluid, nanofluid, hybrid nanofluid, solid nanoparticle  $Al_2O_3$ , and solid nanoparticle  $Cu$ . The thermophysical properties of hybrid nanofluid utilized in Eq. (2) and Eq. (3) are presented in Table 1. Note that the volume fractions of  $Al_2O_3$  and  $Cu$  are symbolized by  $\varphi_{Al_2O_3}$  and  $\varphi_{Cu}$ , respectively. On the other hand, the thermophysical properties of the base fluid (water/ $H_2O$ ) and nanoparticles ( $Al_2O_3$  and  $Cu$ ) are shown in Table 2.

**Table 1**  
 Thermophysical properties of hybrid nanofluid [27,37]

Names	Properties
Dynamic Viscosity	$\mu_{hnf} = \frac{\mu_f}{(1 - \varphi_{Cu})^{5/2} (1 - \varphi_{Al_2O_3})^{5/2}}$
Thermal expansion coefficient	$(\beta)_{hnf} = (1 - \varphi_{Cu}) [(1 - \varphi_{Al_2O_3})(\beta)_f + \varphi_{Al_2O_3}(\beta)_{Al_2O_3}] + \varphi_{Cu}(\beta)_{Cu}$
Density	$\rho_{hnf} = (1 - \varphi_{Cu}) [(1 - \varphi_{Al_2O_3})\rho_f + \varphi_{Al_2O_3}\rho_{Al_2O_3}] + \varphi_{Cu}\rho_{Cu}$
Thermal conductivity	$k_{hnf} = \frac{k_{Cu} + 2k_{nf} - 2\varphi_{Cu}(k_{nf} - k_{Cu})}{k_{Cu} + 2k_{nf} + \varphi_{Cu}(k_{nf} - k_{Cu})} \times (k_{nf}), \text{ where } k_{nf} = \frac{k_{Al_2O_3} + 2k_f - 2\varphi_{Al_2O_3}(k_f - k_{Al_2O_3})}{k_{Al_2O_3} + 2k_f + \varphi_{Al_2O_3}(k_f - k_{Al_2O_3})} \times (k_f)$
Heat capacity	$(\rho c_p)_{hnf} = (1 - \varphi_{Cu}) [(1 - \varphi_{Al_2O_3})(\rho c_p)_f + \varphi_{Al_2O_3}(\rho c_p)_{Al_2O_3}] + \varphi_{Cu}(\rho c_p)_{Cu}$
Electrical conductivity	$\sigma_{hnf} = \frac{\sigma_{Cu} + 2\sigma_{nf} - 2\varphi_{Cu}(\sigma_{nf} - \sigma_{Cu})}{\sigma_{Cu} + 2\sigma_{nf} + \varphi_{Cu}(\sigma_{nf} - \sigma_{Cu})} \times (\sigma_{nf}), \text{ where } (\sigma_{nf}) = \frac{\sigma_{Al_2O_3} + 2\sigma_f - 2\varphi_{Al_2O_3}(\sigma_f - \sigma_{Al_2O_3})}{\sigma_{Al_2O_3} + 2\sigma_f + \varphi_{Al_2O_3}(\sigma_f - \sigma_{Al_2O_3})} \times (\sigma_f)$

**Table 2**  
 Thermophysical properties of copper, alumina and water [27,37]

	$\rho$ (kgm <sup>-3</sup> )	$\sigma$ (Sm <sup>-1</sup> )	$c_p$ (Jkg <sup>-1</sup> K <sup>-1</sup> )	$\beta \times 10^{-5}$ (K <sup>-1</sup> )	$k$ (Wm <sup>-1</sup> K <sup>-1</sup> )	$Pr$
Copper (Cu)	8933	5.96×10 <sup>7</sup>	385	1.67	400	-
Alumina (Al <sub>2</sub> O <sub>3</sub> )	3970	3.69×10 <sup>7</sup>	765	0.85	40	-
Water (H <sub>2</sub> O)	997.1	0.05	4179	21	0.613	6.2

The following similarity variables are considered [37,48,55]

$$u = U_w e^{x/2l} f'(\eta); v = -\sqrt{\frac{U_w \nu_f}{2l}} e^{x/2l} (f(\eta) + \eta f'(\eta)); \theta(\eta) = \frac{T - T_\infty}{T_w - T_\infty}; \eta = y \sqrt{\frac{U_w}{2\nu_f l}} e^{x/2l}. \quad (8)$$

As Eq. (1) is fully satisfied, Eq. (2) and Eq. (3) can be converted to ordinary differential equations (ODEs) by using the similarity variables in Eq. (8) as shown below

$$\frac{\mu_{hnf}/\mu_f}{\rho_{hnf}/\rho_f} f'''' + f'' f - 2(f')^2 + 2\lambda_1 \left( \frac{\beta_{hnf}}{\beta_f} \right) \theta - \frac{\sigma_{hnf}/\sigma_f}{\rho_{hnf}/\rho_f} M f' = 0, \quad (9)$$

$$\frac{1}{Pr(\rho c_p)_{hnf}/(\rho c_p)_f} \left[ \frac{k_{hnf}}{k_f} + \frac{4}{3} Rd \right] \theta'' + \theta' f - 4\theta f' + \frac{\sigma_{hnf}/\sigma_f}{(\rho c_p)_{hnf}/(\rho c_p)_f} MEc (f'^2) = 0. \quad (10)$$

Similarly, the boundary conditions in Eq. (4) and Eq. (5) can be converted using the similarity variables in Eq. (8) and yield the following results

$$f(0) = S, f'(0) = -1 + \delta f''(0), \theta(0) = 1 + \delta_T \theta'(0), \quad (11)$$

$$f'(\eta) \rightarrow 0; \theta(\eta) \rightarrow 0 \text{ as } \eta \rightarrow \infty. \quad (12)$$

The parameters  $M = \frac{2lB_0^2 \sigma_f}{U_w \rho_f}$ ,  $\lambda_1 = \frac{g\beta_f T_0 l}{U_w^2}$ ,  $Pr = \frac{\mu_f (c_p)_f}{k_f}$ ,  $Rd = \frac{4\sigma_1 T_\infty^3}{k^1 k_f}$ , and  $Ec = \frac{u_w^2}{(T_w - T_\infty)(c_p)_f}$  are the magnetic parameter, mixed convection parameter, Prandtl number, thermal radiation parameter, and Eckert number, respectively. Additionally,  $\delta = \zeta_1 \left( \frac{\nu_f U_w}{2l} \right)^{1/2}$  and  $\delta_T = \xi_1 \left( \frac{\nu_f U_w}{2l} \right)^{1/2}$  are the velocity and thermal slip parameters, respectively.

The skin friction coefficient  $C_f$  and the local Nusselt number  $Nu_x$  are then defined as

$$C_f = \frac{\mu_{hnf}}{\rho_f u_w^2} (u_y)_{y=0}, Nu_x = \frac{2l}{k_f (T_w - T_\infty)} \left[ -k_{hnf} (T_y)_{y=0} + (q_r)_{y=0} \right]. \quad (13)$$

The following equations are obtained by employing Eq. (8) and Eq. (13)

$$(Re_x)^{1/2} C_f = \frac{\mu_{hnf}}{\mu_f} f''(0), (Re_x)^{-1/2} Nu_x = - \left[ \frac{k_{hnf}}{k_f} + \frac{4Rd}{3} \right] \theta'(0), \quad (14)$$

where  $Re_x = \frac{2u_w l}{\nu_f}$  is the local Reynolds number.

## 2.2 Numerical Method

The bvp4c solver which runs on the MATLAB computational platform, is employed to solve the system of higher-order nonlinear ODEs described in Eq. (9) and Eq. (10) with the boundary conditions in Eq. (11) and Eq. (12) numerically. Numerous experts and researchers had used the bvp4c solver technique to solve fluid flow problems extensively. The bvp4c algorithm is a finite difference scheme that utilizes the three-stage Lobatto IIIA implicit Runge–Kutta method that yields fourth-order

numerical solutions [62]. We followed the procedures below to incorporate the bvp4c solver into our physical model.

STEP 1: Define new variables for the system of nonlinear higher order (ODEs) in Eq. (9) and Eq. (10).

$$y(1) = f, y(2) = f', y(3) = f'', y(4) = \theta, y(5) = \theta'. \quad (15)$$

STEP 2: By using the new variables defined in Eq. (15), the system of higher-order nonlinear ODEs in Eq. (9) and Eq. (10) can be reduced to a system of first-order nonlinear ODEs as shown below

$$\begin{aligned} f' &= y(2), \\ f'' &= y(3), \\ f''' &= \left[ 2(y(2))^2 - y(1)y(3) - 2\lambda_1(\beta_{hnf}/\beta_f)y(4) + \frac{\sigma_{hnf}/\sigma_f}{\rho_{hnf}/\rho_f} My(2) \right] \frac{\rho_{hnf}/\rho_f}{\mu_{hnf}/\mu_f}, \\ \theta' &= y(5), \\ \theta'' &= \frac{Pr(\rho_{cp})_{hnf}/(\rho_{cp})_f}{(k_{hnf}/k_f + 4Rd/3)} \left[ 4y(2)y(4) - y(1)y(5) - \frac{\sigma_{hnf}/\sigma_f}{(\rho_{cp})_{hnf}/(\rho_{cp})_f} MEc(y(2))^2 \right]. \end{aligned} \quad (16)$$

STEP 3: The boundary conditions in Eq. (11) and Eq. (12) can be expressed in terms of the new variables in Eq. (15)

$$\begin{aligned} y(1)_a &= S, y(2)_a = -1 + \delta y(3)_a, y(4)_a = 1 + \delta_T * y(5)_a, \\ y(2)_b &= 0, y(4)_b = 0. \end{aligned} \quad (17)$$

The subscript 'a' indicates the position of a sheet at  $\eta = 0$  whereas the subscript 'b' represents the location away from the sheet for a certain value of  $\eta$ . We used a value of  $\eta = 20$  for this study.

STEP 4: Programme the system of first-order nonlinear ODEs in Eq. (16) and the boundary conditions in Eq. (17) in bvp4c solver.

STEP 5: Obtain dual solutions by providing two separate initial guesses to the bvp4c solver, one at a time. The first solution can be gained with less restrictive initial guesses, but this is not always true when getting the second solution. This procedure is continued until the numerical solutions asymptotically satisfy the boundary conditions at infinity (i.e., Eq. (12)).

### 3. Results and Discussion

To validate the accuracy of the proposed physical model and algorithm, the current results are compared with those equivalent findings obtained from preceding research. Table 3 shows the values of  $f''(0)$  and  $-\theta'(0)$  under various values of  $Pr$  when  $\varphi_{Al_2O_3} = \varphi_{Cu} = \delta = \delta_T = M = Ec = Rd = 0$ ,  $\lambda_1 = -0.5$ , and  $S = 5$ . These values are compared with those obtained from Waini *et al.*, [48] and Lund *et al.*, [63]. It is noticed that current findings found comparable with those findings obtained by Waini *et al.*, [48] and Lund *et al.*, [63]. On the other hand, Table 4 compares the values of  $f''(0)$  with those found in Hafidzuddin *et al.*, [64], Ghosh and Mukhopadhyay [65], Waini *et al.*, [37], and Yashkun *et al.*, [27], for  $\varphi_{Al_2O_3} = \varphi_{Cu} = \lambda_1 = \delta = \delta_T = M = Ec = Rd = 0$ ,  $S = 3$  and  $Pr = 0.7$ . An outstanding agreement among the values of  $f''(0)$  can be seen in Table 4.

**Table 3**

Values of  $f''(0)$  and  $-\theta'(0)$  for several values of  $Pr$  when  $\varphi_{Al_2O_3} = \varphi_{Cu} = \delta = \delta_T = M = Ec = Rd = 0, \lambda_1 = -0.5$ , and  $S = 5$

$Pr$	Waini <i>et al.</i> , [48]		Lund <i>et al.</i> , [63]		Current Study	
	$f''(0)$	$-\theta'(0)$	$f''(0)$	$-\theta'(0)$	$f''(0)$	$-\theta'(0)$
1	4.449204	4.447507	4.449203	4.447507	4.4492038	4.4475074
1.6	4.540536	7.334578	4.540536	7.334577	4.5405362	7.3345777
2	4.570373	9.284829	4.570372	9.284828	4.5703728	9.2848287
2.4	4.590011	11.247348	4.590011	11.247347	4.5900111	11.2473478
3.5	-	-	-	-	4.6203020	16.6805390
4.5	-	-	-	-	4.6346512	21.6444129
5.5	-	-	-	-	4.6436342	26.6201308
6.2	4.648147	30.107416	-	-	4.6481472	30.1074164

**Table 4**

Values of  $f''(0)$  when  $\varphi_{Al_2O_3} = \varphi_{Cu} = \lambda_1 = \delta = \delta_T = M = Ec = Rd = 0, S = 3$ , and  $Pr = 0.7$

	First solution, $f''(0)$	Second solution, $f''(0)$
Hafidzuddin <i>et al.</i> , [64]	2.3908	-0.9722
Ghosh and Mukhopadhyay [65]	2.39082	-0.97223
Waini <i>et al.</i> , [37]	2.390814	-0.972247
Yashkun <i>et al.</i> , [27]	2.390813	-0.972247
Current Study	2.3908165	-0.9722473

The effect of various parameters on reduced skin friction  $f''(0)$  and reduced heat transfer  $-\theta'(0)$  are depicted in Figure 2 to Figure 6, while the velocity profile  $f'(\eta)$  and temperature profile  $\theta(\eta)$  are shown in Figure 7 to Figure 16. The reduced skin friction  $f''(0)$  and reduced heat transfer  $-\theta'(0)$  are considered to determine the shear stress and heat transfer rate on the boundary layer surface, respectively. On the other hand, velocity profile  $f'(\eta)$  and temperature profile  $\theta(\eta)$  show interest in boundary layer thickness on momentum and thermal boundary layers, respectively. Figure 2 and Figure 3 depict the variation of  $f''(0)$  and  $-\theta'(0)$  with respect to  $S$ , respectively, using three fixed values of  $\varphi_{Cu} = 0, 0.04, 0.08$  with parameters  $\varphi_{Al_2O_3} = 0.01; Pr = 6.2; \delta = \delta_T = 0.1; M = Rd = 0.01; \lambda_1 = -0.5$ ; and  $Ec = 0.1$ . This study chooses  $\varphi_{Cu}$  values ranging from 0 to 0.08, which was shown to be suitable within the range of  $\varphi_{Cu}$  previously explored by Yan *et al.*, [55] (i.e.,  $0 \leq \varphi_{Cu} \leq 0.1$ ). It's worth mentioning that the hybrid nanofluid flows until it reaches  $S_{ci}, i = 1, 2, 3$ .  $S_{ci}$  is the critical point of  $S$  where both solutions meet each other. Dual solutions exist when  $S \geq S_{ci}$ . No solutions exist when  $S < S_{ci}$ . Furthermore, when  $\varphi_{Cu} = 0$ , it is purely  $Al_2O_3$ /water-based nanofluid and  $S_{c1} = 1.9503$ . Subsequently, if 4% of  $\varphi_{Cu}$  is added, then  $S_{c2} = 1.8650$ . Moreover,  $S_{c3} = 1.7870$  is obtained as a result of adding 8% of  $\varphi_{Cu}$ . In Figure 2, the value of  $f''(0)$  upsurges in the first solution and declines in the second solution as the value of  $\varphi_{Cu}$  rises. From Figure 3, it is noticed the value of  $-\theta'(0)$  drops in both solutions when  $\varphi_{Cu}$  is enhanced. The addition of  $\varphi_{Cu}$  extended the boundary layer separation physically. This also showed that a sufficient suction strength is required to maintain flow along a shrinking sheet. The same findings were reported by Waini *et al.*, [48].

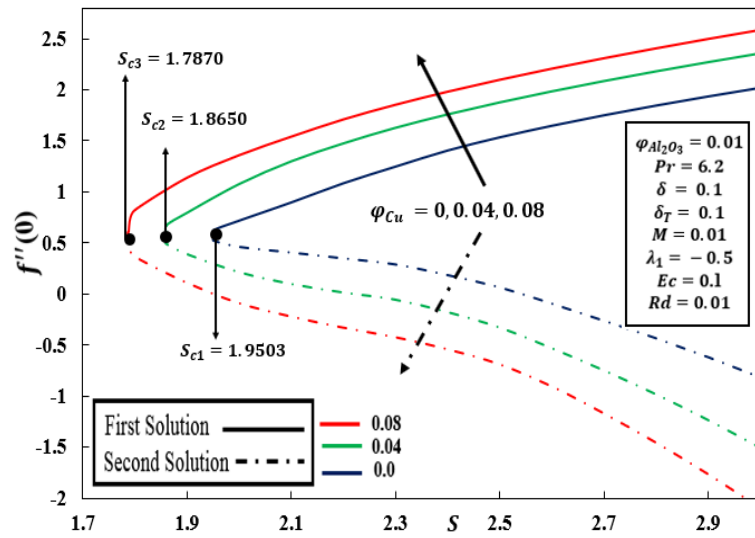


Fig. 2. Influence of  $\varphi_{Cu}$  on  $f''(0)$

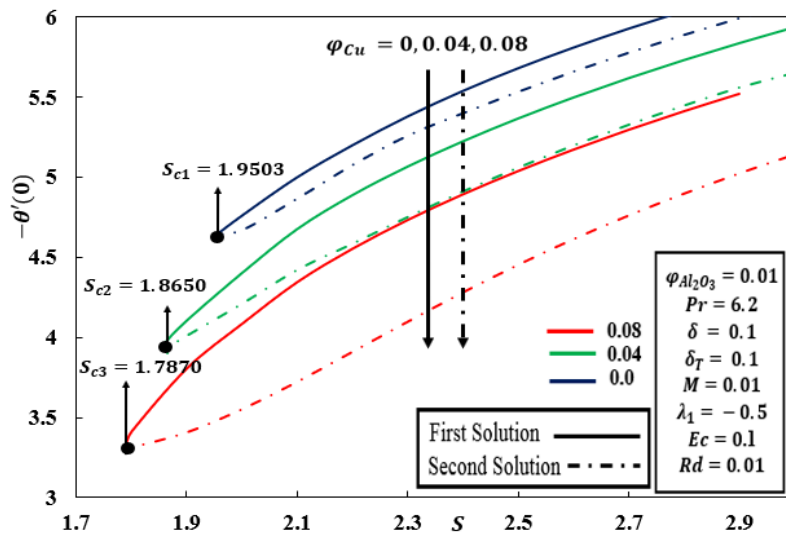


Fig. 3. Influence of  $\varphi_{Cu}$  on  $-\theta'(0)$

Figure 4 and Figure 5 demonstrate the effect of mixed convection parameter  $\lambda_1 = -0.5, -0.3, -0.1$  on the reduced skin friction  $f''(0)$  and reduced heat transfer  $-\theta'(0)$  with respect to the parameter  $S$  when  $\varphi_{Al_2O_3} = 0.01$ ,  $\varphi_{Cu} = 0.08$ ,  $Pr = 6.2$ ,  $\delta = \delta_T = 0.1$ ,  $M = Rd = 0.01$ , and  $Ec = 0.1$ , respectively. The chosen values of mixed convection parameter  $\lambda_1$  in Figure 4 and Figure 5 are inside the range of  $\lambda_1 \in [-1, 1]$  as recommended by Waini *et al.*, [48]. Dual solutions are noticed in the suction region when  $S_{c1} = 1.7870$ ,  $S_{c2} = 1.8401$  and  $S_{c3} = 1.9001$  are critical points against  $\lambda_1 = -0.5, -0.3, -0.1$ , respectively. According to Figure 4, both solutions of  $f''(0)$  are enhanced when the value of mixed convection  $\lambda_1$  is increased. Moreover, in Figure 5, it can be seen that the first solution of  $-\theta'(0)$  does not vary significantly, but only the second solution rises as the value of mixed convection parameter  $\lambda_1$  being raised from  $-0.5$  to  $-0.1$ . Therefore, the assisted flow is possible on the physical surface. Similar result can be seen in Waini *et al.*, [52].

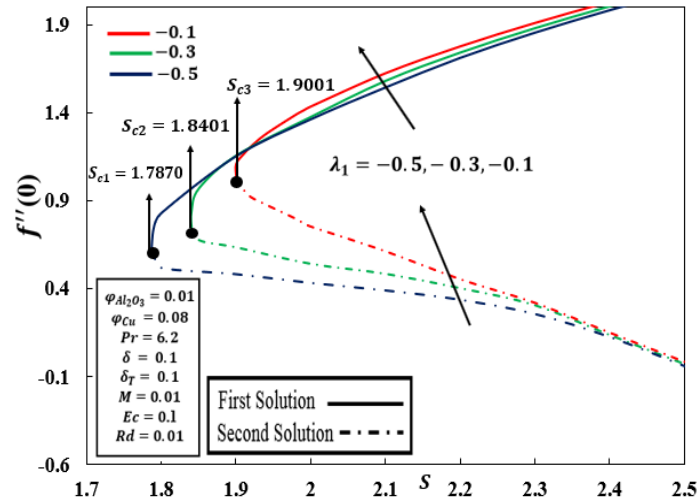


Fig. 4. Influence of  $\lambda_1$  on  $f''(0)$

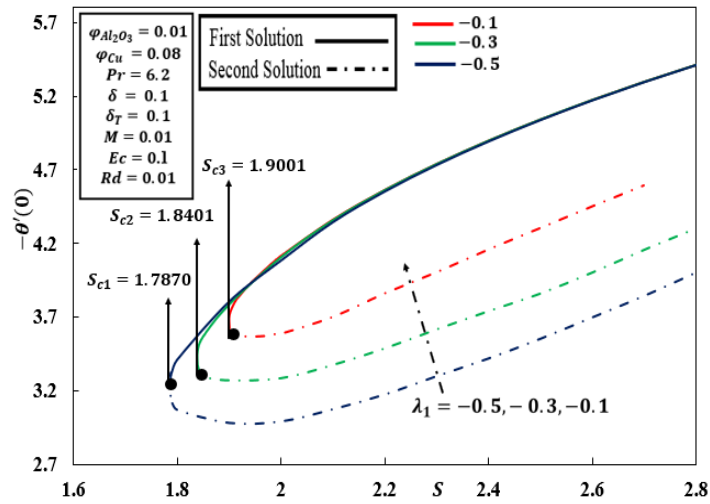


Fig. 5. Influence of  $\lambda_1$  on  $-\theta'(0)$

Figure 6 portrays the influence of radiation  $Rd = 0.01, 0.05, 0.1$  with respect to  $S$  on the reduced heat transfer  $-\theta'(0)$  using the setting  $\varphi_{Al_2O_3} = 0.01, \varphi_{Cu} = 0.04, Pr = 6.2, \delta = \delta_T = 0.1, M = 0.01, \lambda_1 = -0.5$ , and  $Ec = 0.1$ . Radiation parameter  $Rd$  only occurs in Eq. (3). Consequently, the values of  $Rd$  have no influence on  $f''(0)$  since it is uncoupled from the momentum Eq. (2). In Figure 6, it is seen that the magnitude of reduced heat transfer  $-\theta'(0)$  drops in both solutions as the value of radiation  $Rd$  rises. For all quantities of  $Rd$ , the critical value is revealed to be equal i.e.,  $S_c = 1.8650$ . It is worth to declare that the dual solutions happen when  $S < S_c$ , and no solution occurs beyond  $S_c$ . Physically, it means that higher radiation  $Rd$  reduces the rate of heat transfer at the surface. These similar conclusions were also reported in Anuar *et al.*, [43].

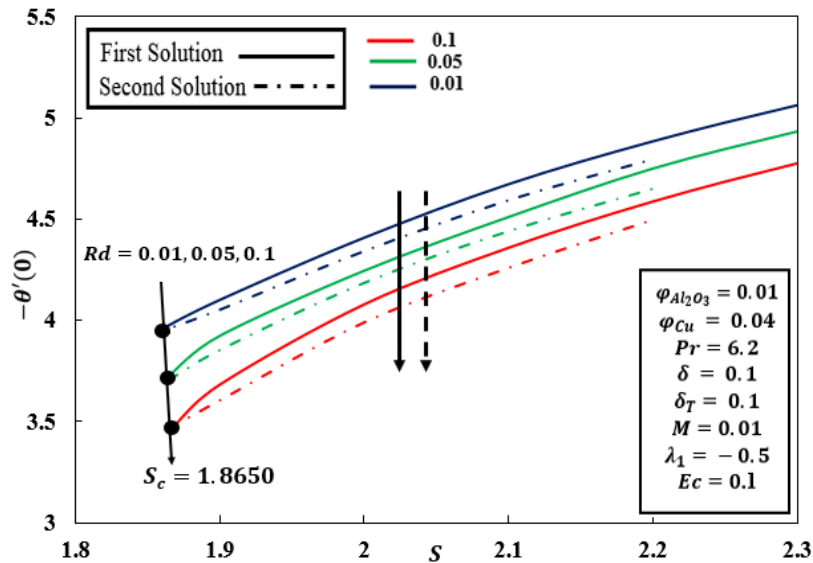


Fig. 6. Influence of  $Rd$  on  $-\theta'(0)$

On the other hand, Figure 7 illustrates the influence of  $Rd = 0.01, 0.03, 0.05$  on the temperature profile  $\theta(\eta)$  using the setting  $\varphi_{Al_2O_3} = \varphi_{Cu} = 0.01, Pr = 6.2, \delta = 0.1, \delta_T = 0.2, S = 3, \lambda_1 = -0.1, M = 0.01,$  and  $Ec = 0.1$ . The thickness of the thermal boundary layer grows with increasing values of  $Rd$  in both solutions, hence, indicating physically that larger  $Rd$  values result in a lower temperature gradient at the surface of the sheet. Due to the occurrence of extreme radiation, a massive quantity of heat energy is generated in the system, which reasons the temperature of the fluid  $\theta(\eta)$  to rise. Similar findings in the temperature profile  $\theta(\eta)$  can also be observed in Lund *et al.*, [36] and Waini *et al.*, [37]. The radiation parameter  $Rd$  picked to generate the results in Figure 7 and Figure 8 are within the range of  $Rd \in [0,1]$  proposed by Waini *et al.*, [37].

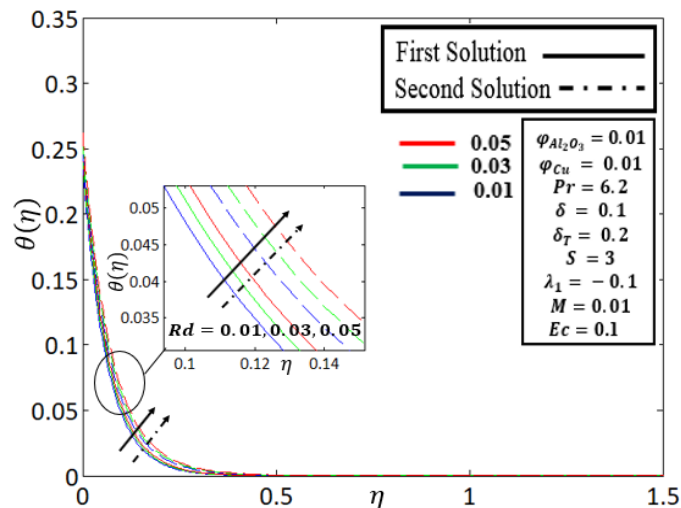


Fig. 7. Influence of  $Rd$  on  $\theta(\eta)$

The graphs of velocity profile  $f'(\eta)$  and temperature profile  $\theta(\eta)$  for solid volume fraction  $\varphi_{Al_2O_3} = 0.01, 0.02, 0.03$  are shown in Figure 8 and Figure 9, respectively. This study selects the  $\varphi_{Al_2O_3}$  parameter values to go between 0.01 and 0.03, which was noticed to be acceptable inside a wider range value of the  $\varphi_{Al_2O_3}$  parameter previously used by Yan *et al.*, [55] (i.e.,  $0 \leq \varphi_{Al_2O_3} \leq 0.07$ ). In Figure 8, it is found that both solutions reduce with the growing values of  $\varphi_{Al_2O_3}$ . Besides,

in Figure 9, both solutions are upsurgings when  $\varphi_{Al_2O_3}$  is enhanced, but the opposite tendency takes place subsequently for  $\eta > 0.6$ . In terms of physical significance on the surface, the thickness of the momentum boundary layer reduced while the thickness of the thermal boundary layer enhanced. Yan *et al.*, [55] observed similar findings.

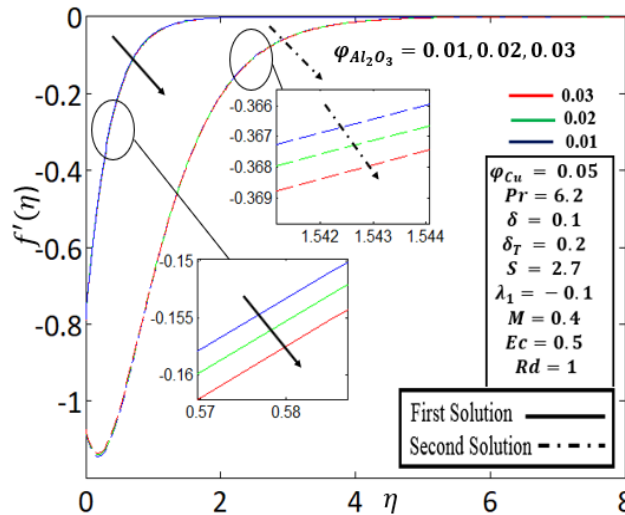


Fig. 8. Influence of  $\varphi_{Al_2O_3}$  on  $f'(\eta)$

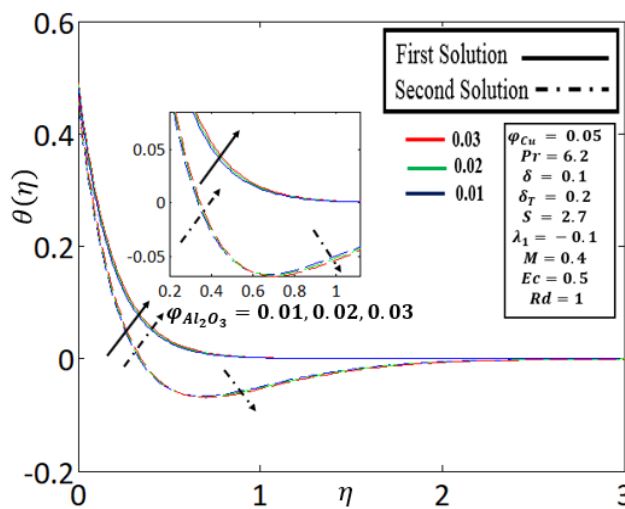


Fig. 9. Influence of  $\varphi_{Al_2O_3}$  on  $\theta(\eta)$

Figure 10 and Figure 11 portray the influence of various velocity slip parameters  $\delta = 0.1, 0.3, 0.5$  on the velocity  $f'(\eta)$  and temperature  $\theta(\eta)$  profiles, respectively using  $\varphi_{Al_2O_3} = 0.1$ ,  $\varphi_{Cu} = 0.02$ ,  $Pr = 6.2$ ,  $\delta_T = 0.1$ ,  $S = 2.7$ ,  $\lambda_1 = -0.3$ ,  $M = 0.01$ ,  $Ec = 0.1$ , and  $Rd = 0.1$ . These investigations choose a range of 0.1 to 0.5 for the velocity parameter  $\delta$ , which was shown to be acceptable within the range of values for the same parameter previously used in Hayat *et al.*, [58] (i.e.,  $0 \leq \delta \leq 2$ ). From Figure 10, the increasing behaviour of the velocity profile  $f'(\eta)$  for both solutions are noticed when improving the values of  $\delta$ . Moreover, from Figure 11, the decreasing behaviour of the first solution and the increasing behaviour of the second solution for temperature profile  $\theta(\eta)$  are observed when enhancing the values of  $\delta$ . Physically, it is pragmatic that no-slip condition (when  $\delta = 0$ ) has a lower effect on the boundary layer separation than the occurrence of velocity slip  $\delta$  in the hybrid nanofluid. Hayat *et al.*, [58] also obtained this similar finding.

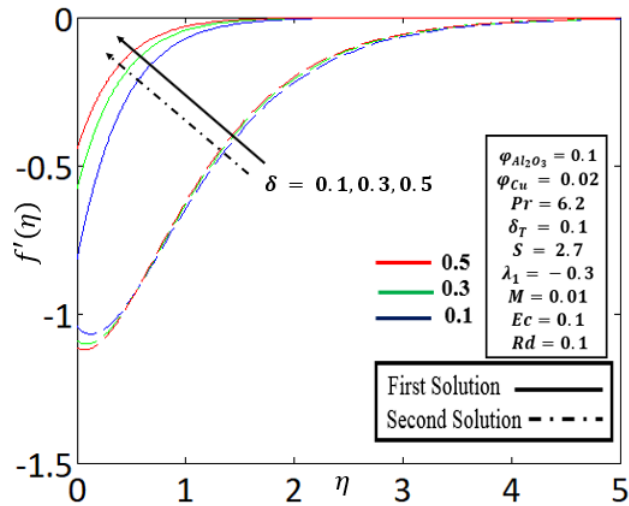


Fig. 10. Influence of  $\delta$  on  $f'(\eta)$

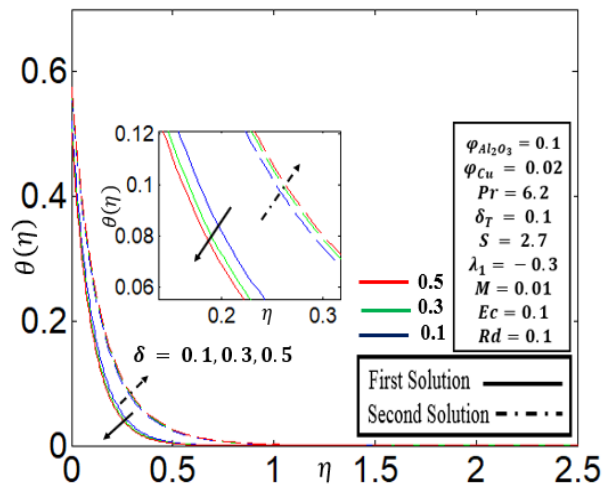


Fig. 11. Influence of  $\delta$  on  $\theta(\eta)$

Figure 12 and Figure 13 continue to study on the behaviour of the velocity  $f'(\eta)$  and temperature  $\theta(\eta)$  profiles, respectively, for various values of the thermal slip parameter  $\delta_T = 0.1, 0.3, 0.5$ . Parameters that are fixed in these investigations are  $\varphi_{Al_2O_3} = 0.1, \varphi_{Cu} = 0.02, Pr = 6.2, \delta_T = 0.1, S = 2.7, \lambda_1 = -0.3, M = 0.01, Ec = 0.1,$  and  $Rd = 0.1$ . This study picks the thermal slip parameter to vary between the values of 0.1 and 0.5, which fall within a wider range of thermal slip parameter  $\delta_T$  suggested by Hayat *et al.*, [58] (i.e.,  $0 \leq \delta_T \leq 2$ ). Based on Figure 12, it is observed that the velocity of the first solution increases along with the increment of the values of  $\delta_T$ , but an opposite trend is spotted for the velocity of the second solution. On the other hand, temperature for both solutions decline when increasing the value of the thermal slip  $\delta_T$ , as shown in Figure 13. Physically, it means that when the thermal slip parameter  $\delta_T$  increases, less heat is transferred from the surface to the hybrid nanofluid, and hence lowering the temperature of the fluid. Hayat *et al.*, [58] reported a similar outcome on temperature profile.

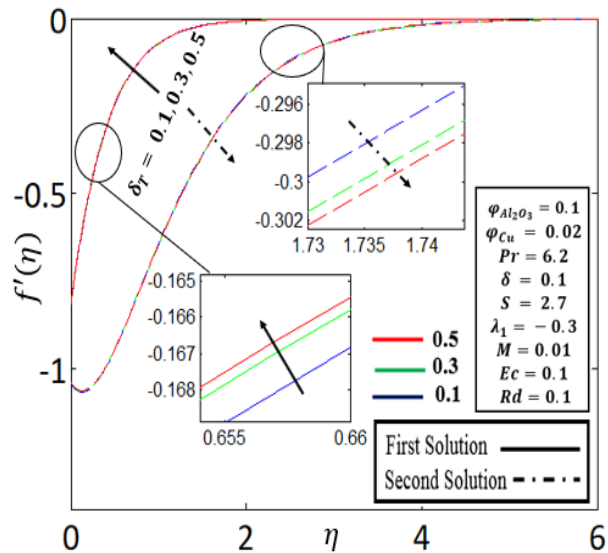


Fig. 12. Influence of  $\delta_T$  on  $f'(\eta)$

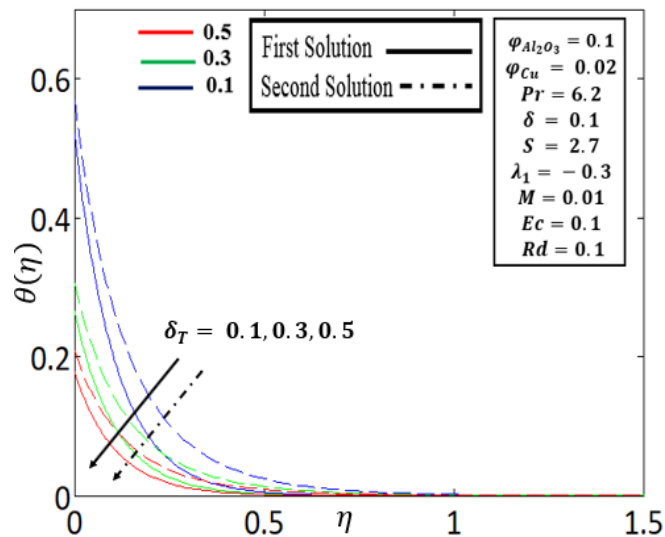


Fig. 13. Influence of  $\delta_T$  on  $\theta(\eta)$

The plots of the velocity profile  $f'(\eta)$  and temperature profile  $\theta(\eta)$  for  $M = 3.0, 4.0, 5.0$  are represented in Figure 14 and Figure 15, respectively. The different quantities of  $M$  utilised in Figure 14 and Figure 15 are very frequent used in the literature as Aly and Pop [39] employed a larger range of  $M$  (i.e.,  $1 \leq M \leq 10$ ) in their research. As seen in Figure 14, the velocity profile  $f'(\eta)$  grows in the first solution but falls in the second solution, indicating the rate of movement significantly decreases as  $M$  rises. This is owing to the Lorentz force created by the physical magnetic field, which caused the movement mechanism to be more resistant. As a result,  $M$  decreases the shear stress of the surface. Moreover, temperature for both first and second solution increases along with a rising value of  $M$ , as noticed in Figure 15. Similar outcome has been observed in the work of Yashkun *et al.*, [27].

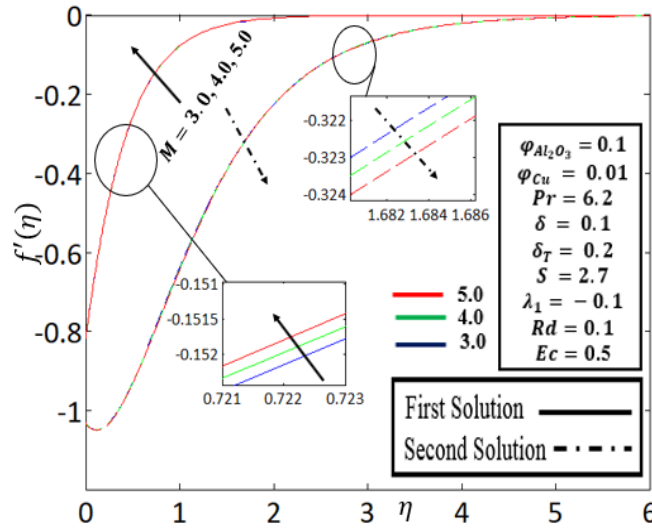


Fig. 14. Influence of  $M$  on  $f'(\eta)$

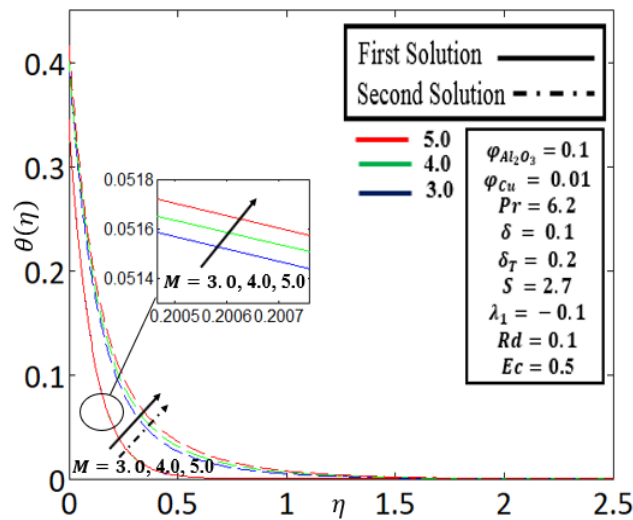


Fig. 15. Influence of  $M$  on  $\theta(\eta)$

By setting  $\varphi_{Al_2O_3} = 0.1$ ,  $\varphi_{Cu} = 0.05$ ,  $Pr = 6.2$ ,  $\delta = 0.1$ ,  $\delta_T = 0.2$ ,  $S = 2.5$ ,  $\lambda_1 = -0.1$ ,  $M = 0.1$ , and  $Rd = 0.01$ , the temperature profile  $\theta(\eta)$  for the values of Eckert number  $Ec = 0, 0.5, 1$  is illustrated in Figure 16. This study chooses the Eckert number  $Ec$  ranging from 0 to 1, following the similar choice previously applied in Khashi'ie *et al.*, [54] (i.e.,  $0.01 \leq Ec \leq 1$ ). Figure 16 has witnessed an increment in the temperature of both first and second solution when the value of  $Ec$  is increased. This indicates physically that the strength of heat transfer grows as the quantity of  $Ec$  increases due to the increasing heat created by Joule heating. The result shown in Figure 16 agreed with the finding obtained by Asghar and Ying [33].

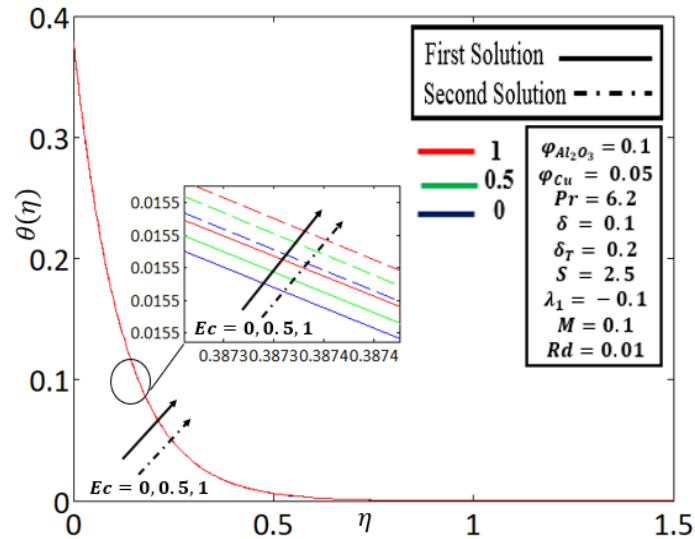


Fig. 16. Influence of  $Ec$  on  $\theta(\eta)$

#### 4. Conclusions

This paper has proposed a two-dimensional magnetized and mixed convection  $Al_2O_3$ -Cu/ $H_2O$  hybrid nanofluid flow with thermal radiation, Joule heating, velocity and thermal slip conditions over an exponential vertical shrinking sheet. This study has investigated the behaviour of the reduced skin friction  $f''(0)$ , reduced heat transfer  $-\theta'(0)$ , velocity and temperature profiles of hybrid nanofluid under the influence of suction/injection, MHD, mixed convection, Joule heating, thermal radiation, velocity and thermal slip conditions. The physical model proposed in this study has been validated. All numerical and graphical results have been obtained by solving the system of higher-order nonlinear ODEs and its corresponding boundary conditions using the bvp4c solver which runs on the MATLAB computing platform. The main conclusions of the present study are as follows

- i. Multiple solutions are proved to be possible given a reasonable set of specified parameters.
- ii. The hybrid nanofluid continues to flow until it reaches a critical point  $S_{ci}$  such that  $S \geq S_{ci}$ , while no fluid flow is possible for  $S < S_{ci}$ .
- iii. The inclusion of hybrid nanoparticles has raised the heat transfer rate.
- iv. The addition of  $\varphi_{Cu}$  prolonged the boundary layer separation.
- v. When the mixed convection parameter  $\lambda_1$  is enhanced, the value of  $f''(0)$  also increased in both solutions.
- vi. The value of  $-\theta'(0)$  upsurged in the second solution but no variation is observed in the first solution when the mixed convection parameter  $\lambda_1$  is increased.
- vii. The temperature profile  $\theta(\eta)$  increased in both solutions when enhancing the parameters  $Rd, M, Ec$ , and solid volume fraction  $\varphi_{Al_2O_3}$ .
- viii. The temperature profile  $\theta(\eta)$  decreased in both solutions as thermal slip parameter  $\delta_T$  increased. However, when the velocity slip parameter  $\delta$  is enhanced, temperature profile declined in the first solution but upsurged in the second solution.

This study is motivated by the many useful applications of hybrid nanofluid. This study has revealed several previously unknown behaviour of hybrid nanofluid under the combined influence of Joule heating, thermal radiation, velocity and thermal slip conditions, magnetic field, and mixed

convection when it flows across a vertical exponentially shrinking sheet. Such physical situation has not been examined in the existing literature. The suggested model has the potential to be used in the air conditioning system. The hybrid nanofluid which acts as the refrigerant is circulated throughout the air conditioning system by a compressor. At specific point, the hot refrigerant will pass through the micro heat exchanger where slip condition occurs to decrease the fluid flow's resistance. A fan which comprises a spinning motor powered by magnetic field, is installed near the micro heat exchanger. The fan will blow towards the exchanger so that heat from the hot refrigerant can be transferred to the surrounding air through mixed convection. The surrounding warm air will then be released outside the building through radiation. The air conditioning system has an overload protector, which prevents the air conditioning system from overheating. Consequently, Joule heating happened as the overload protector works as a resistor.

Finally, various recommendations for future studies include updating the present proposed model utilizing other types of physical parameters such as viscous heating, heat source/absorption, and thermal convective condition, or reconsidering the proposed model in three-dimensional space.

### Acknowledgement

This research was not funded by any grant.

### References

- [1] Sakiadis, B. C. "Boundary - layer behavior on continuous solid surfaces: I. Boundary - layer equations for two - dimensional and axisymmetric flow." *AIChE Journal* 7 (1961): 26-28. <https://doi.org/10.1002/aic.690070108>
- [2] Crane, Lawrence J. "Flow past a stretching plate." *Zeitschrift für angewandte Mathematik und Physik ZAMP* 21, no. 4 (1970): 645-647. <https://doi.org/10.1007/BF01587695>
- [3] Choi, S. US, and Jeffrey A. Eastman. *Enhancing thermal conductivity of fluids with nanoparticles*. No. ANL/MSD/CP-84938; CONF-951135-29. Argonne National Lab.(ANL), Argonne, IL (United States), 1995.
- [4] Lund, Liaquat Ali, Zurni Omar, Sumera Dero, Dumitru Baleanu, and Ilyas Khan. "Rotating 3D flow of hybrid nanofluid on exponentially shrinking sheet: Symmetrical solution and duality." *Symmetry* 12, no. 10 (2020): 1637. <https://doi.org/10.3390/sym12101637>
- [5] Miklavčič, M., and C. Wang. "Viscous flow due to a shrinking sheet." *Quarterly of Applied Mathematics* 64, no. 2 (2006): 283-290. <https://doi.org/10.1090/S0033-569X-06-01002-5>
- [6] Qayyum, Sumaira, Muhammad Ijaz Khan, Tasawar Hayat, and Ahmed Alsaedi. "A framework for nonlinear thermal radiation and homogeneous-heterogeneous reactions flow based on silver-water and copper-water nanoparticles: a numerical model for probable error." *Results in Physics* 7 (2017): 1907-1914. <https://doi.org/10.1016/j.rinp.2017.05.020>
- [7] Ahmad, Syakila, and Ioan Pop. "Mixed convection boundary layer flow from a vertical flat plate embedded in a porous medium filled with nanofluids." *International Communications in Heat and Mass Transfer* 37, no. 8 (2010): 987-991. <https://doi.org/10.1016/j.icheatmasstransfer.2010.06.004>
- [8] Khan, M. Waleed Ahmed, M. Ijaz Khan, T. Hayat, and A. Alsaedi. "Entropy generation minimization (EGM) of nanofluid flow by a thin moving needle with nonlinear thermal radiation." *Physica B: Condensed Matter* 534 (2018): 113-119. <https://doi.org/10.1016/j.physb.2018.01.023>
- [9] Magyari, E., and B. Keller. "Heat and mass transfer in the boundary layers on an exponentially stretching continuous surface." *Journal of Physics D: Applied Physics* 32, no. 5 (1999): 577. <https://doi.org/10.1088/0022-3727/32/5/012>
- [10] Elbashareshy, E. M. A. "Heat transfer over an exponentially stretching continuous surface with suction." *Archives of Mechanics* 53, no. 6 (2001): 643-651.
- [11] Khan, Ansab Azam, Khairy Zaimi, Suliadi Firdaus Sufahani, and Mohammad Ferdows. "MHD flow and heat transfer of double stratified micropolar fluid over a vertical permeable shrinking/stretching sheet with chemical reaction and heat source." *Journal of Advanced Research in Applied Sciences and Engineering Technology* 21, no. 1 (2020): 1-14. <https://doi.org/10.37934/araset.21.1.114>
- [12] Dero, Sumera, Azizah Mohd Rohni, and Azizan Saaban. "Triple Solutions and Stability Analysis of Mixed Convection Boundary Flow of Casson Nanofluid over an Exponentially Vertical Stretching/Shrinking Sheet." *Journal of Advanced Research in Fluid Mechanics and Thermal Sciences* 72, no. 1 (2020): 94-110. <https://doi.org/10.37934/arfmts.72.1.94110>

- [13] Dzulkipli, Nor Fadhilah, Norfifah Bachok, Nor Azizah Yacob, Ioan Pop, Norihan Arifin, and Haliza Rosali. "Stability Solution of Unsteady Stagnation-Point Flow and Heat Transfer over a Stretching/Shrinking Sheet in Nanofluid with Slip Velocity Effect." *CFD Letters* 14, no. 1 (2022): 66-86. <https://doi.org/10.37934/cfdl.14.1.6686>
- [14] Zokri, Syazwani Mohd, Nur Syamilah Arifin, Abdul Rahman Mohd Kasim, and Mohd Zuki Salleh. "Free convection boundary layer flow of Jeffrey nanofluid on a horizontal circular cylinder with viscous dissipation effect." *Journal of Advanced Research in Micro and Nano Engineering* 1, no. 1 (2020): 1-14. <https://doi.org/10.37934/cfdl.12.11.113>
- [15] Mahat, Rahimah, Muhammad Saqib, Imran Ulah, Sharidan Shafie, and Sharena Mohamad Isa. "MHD Mixed Convection of Viscoelastic Nanofluid Flow due to Constant Heat Flux." *Journal of Advanced Research in Numerical Heat Transfer* 9, no. 1 (2022): 19-25.
- [16] Akaje, T. W., and B. I. Olajuwon. "Impacts of Nonlinear thermal radiation on a stagnation point of an aligned MHD Casson nanofluid flow with Thompson and Troian slip boundary condition." *Journal of Advanced Research in Experimental Fluid Mechanics and Heat Transfer* 6, no. 1 (2021): 1-15.
- [17] Wang, Fuzhang, Tanveer Sajid, Assad Ayub, Zulqurnain Sabir, Saira Bhatti, Nehad Ali Shah, Rahma Sadat, and Mohamed R. Ali. "Melting and entropy generation of infinite shear rate viscosity Carreau model over Riga plate with erratic thickness: a numerical Keller Box approach." *Waves in Random and Complex Media* (2022): 1-25. <https://doi.org/10.1080/17455030.2022.2063991>
- [18] Ayub, Assad, Hafiz A. Wahab, Mohammed Balubaid, S. R. Mahmoud, Mohamed R. Ali, and R. Sadat. "Analysis of the nanoscale heat transport and Lorentz force based on the time-dependent Cross nanofluid." *Engineering with Computers* (2022): 1-20. <https://doi.org/10.1007/s00366-021-01579-1>
- [19] Ayub, Assad, Syed Zahir Hussain Shah, Zulqurnain Sabir, N. Seshagiri Rao, Rahma Sadat, and Mohamed R. Ali. "Spectral relaxation approach and velocity slip stagnation point flow of inclined magnetized cross-nanofluid with a quadratic multiple regression model." *Waves in Random and Complex Media* (2022): 1-25. <https://doi.org/10.1080/17455030.2022.2049923>
- [20] Shah, Syed Latif, Assad Ayub, Sanaullah Dehraj, Hafiz A. Wahab, K. Martin Sagayam, Mohamed R. Ali, Rahma Sadat, and Zulqurnain Sabir. "Magnetic dipole aspect of binary chemical reactive Cross nanofluid and heat transport over composite cylindrical panels." *Waves in Random and Complex Media* (2022): 1-24. <https://doi.org/10.1080/17455030.2021.2020373>
- [21] Ayub, Assad, Zulqurnain Sabir, Syed Zahir Hussain Shah, S. R. Mahmoud, Ali Algarni, R. Sadat, and Mohamed R. Ali. "Aspects of infinite shear rate viscosity and heat transport of magnetized Carreau nanofluid." *The European Physical Journal Plus* 137, no. 2 (2022): 1-17. <https://doi.org/10.1140/epjp/s13360-022-02410-6>
- [22] Sadat, R., Praveen Agarwal, R. Saleh, and Mohamed R. Ali. "Lie symmetry analysis and invariant solutions of 3D Euler equations for axisymmetric, incompressible, and inviscid flow in the cylindrical coordinates." *Advances in Difference Equations* 2021, no. 1 (2021): 1-16. <https://doi.org/10.1186/s13662-021-03637-w>
- [23] Huminic, Gabriela, and Angel Huminic. "Hybrid nanofluids for heat transfer applications-a state-of-the-art review." *International Journal of Heat and Mass Transfer* 125 (2018): 82-103. <https://doi.org/10.1016/j.ijheatmasstransfer.2018.04.059>
- [24] Suresh, S., K. P. Venkitaraj, P. Selvakumar, and M. Chandrasekar. "Synthesis of Al<sub>2</sub>O<sub>3</sub>-Cu/water hybrid nanofluids using two step method and its thermo physical properties." *Colloids and Surfaces A: Physicochemical and Engineering Aspects* 388, no. 1-3 (2011): 41-48. <https://doi.org/10.1016/j.colsurfa.2011.08.005>
- [25] Devi, S. P. Anjali, and S. Suriya Uma Devi. "Numerical investigation of hydromagnetic hybrid Cu-Al<sub>2</sub>O<sub>3</sub>/water nanofluid flow over a permeable stretching sheet with suction." *International Journal of Nonlinear Sciences and Numerical Simulation* 17, no. 5 (2016): 249-257. <https://doi.org/10.1515/ijnsns-2016-0037>
- [26] Waini, Iskandar, Anuar Ishak, and Ioan Pop. "Unsteady flow and heat transfer past a stretching/shrinking sheet in a hybrid nanofluid." *International Journal of Heat and Mass Transfer* 136 (2019): 288-297. <https://doi.org/10.1016/j.ijheatmasstransfer.2019.02.101>
- [27] Yashkun, Ubaidullah, Khairy Zaimi, Anuar Ishak, Ioan Pop, and Rabeb Sidaoui. "Hybrid nanofluid flow through an exponentially stretching/shrinking sheet with mixed convection and Joule heating." *International Journal of Numerical Methods for Heat & Fluid Flow* 31, no. 6 (2020): 1930-1950. <https://doi.org/10.1108/HFF-07-2020-0423>
- [28] Zainal, Nurul Amira, Roslinda Nazar, Kohilavani Naganthran, and Ioan Pop. "Heat generation/absorption effect on MHD flow of hybrid nanofluid over bidirectional exponential stretching/shrinking sheet." *Chinese Journal of Physics* 69 (2021): 118-133. <https://doi.org/10.1016/j.cjph.2020.12.002>
- [29] Asghar, Adnan, Teh Yuan Ying, and Khairy Zaimi. "Two-Dimensional Mixed Convection and Radiative Al<sub>2</sub>O<sub>3</sub>-Cu/H<sub>2</sub>O Hybrid Nanofluid Flow over a Vertical Exponentially Shrinking Sheet with Partial Slip Conditions." *CFD Letters* 14, no. 3 (2022): 22-38. <https://doi.org/10.37934/cfdl.14.3.2238>
- [30] Zainal, N. A., Roslinda Nazar, Kohilavani Naganthran, and Ioan Pop. "Viscous dissipation and MHD hybrid nanofluid flow towards an exponentially stretching/shrinking surface." *Neural Computing and Applications* 33, no. 17 (2021): 11285-11295. <https://doi.org/10.1007/s00521-020-05645-5>

- [31] Wahid, Nur Syahirah, Norihan Md Arifin, Najiyah Safwa Khashi'ie, Ioan Pop, Norfifah Bachok, and Mohd Ezad Hafidz Hafidzuddin. "Flow and heat transfer of hybrid nanofluid induced by an exponentially stretching/shrinking curved surface." *Case Studies in Thermal Engineering* 25 (2021): 100982. <https://doi.org/10.1016/j.csite.2021.100982>
- [32] Anuar, Nur Syazana, Norfifah Bachok, Norihan Md Arifin, and Haliza Rosali. "Effect of suction/injection on stagnation point flow of hybrid nanofluid over an exponentially shrinking sheet with stability analysis." *CFD Letters* 11, no. 12 (2019): 21-33. <https://doi.org/10.3390/sym11040522>
- [33] Ashgar, Adnan, and Teh Yuan Ying. "Three dimensional MHD hybrid nanofluid Flow with rotating stretching/shrinking sheet and Joule heating." *CFD Letters* 13, no. 8 (2021): 1-19. <https://doi.org/10.37934/cfdl.13.8.119>
- [34] Devi, S. Suriya Uma, and S. P. Anjali Devi. "Numerical investigation of three-dimensional hybrid Cu-Al<sub>2</sub>O<sub>3</sub>/water nanofluid flow over a stretching sheet with effecting Lorentz force subject to Newtonian heating." *Canadian Journal of Physics* 94, no. 5 (2016): 490-496. <https://doi.org/10.1139/cjp-2015-0799>
- [35] Devi, Suriya Uma, and SP Anjali Devi. "Heat transfer enhancement of Cu-Al<sub>2</sub>O<sub>3</sub>/water hybrid nanofluid flow over a stretching sheet." *Journal of the Nigerian Mathematical Society* 36, no. 2 (2017): 419-433.
- [36] Lund, Liaquat Ali, Zurni Omar, Ilyas Khan, and El-Sayed M. Sherif. "Dual solutions and stability analysis of a hybrid nanofluid over a stretching/shrinking sheet executing MHD flow." *Symmetry* 12, no. 2 (2020): 276. <https://doi.org/10.3390/sym12020276>
- [37] Waini, Iskandar, Anuar Ishak, and Ioan Pop. "Hybrid nanofluid flow induced by an exponentially shrinking sheet." *Chinese Journal of Physics* 68 (2020): 468-482. <https://doi.org/10.1016/j.cjph.2019.12.015>
- [38] Waini, Iskandar, Anuar Ishak, and Ioan Pop. "MHD flow and heat transfer of a hybrid nanofluid past a permeable stretching/shrinking wedge." *Applied Mathematics and Mechanics* 41, no. 3 (2020): 507-520. <https://doi.org/10.1007/s10483-020-2584-7>
- [39] Aly, Emad H., and Ioan Pop. "MHD flow and heat transfer over a permeable stretching/shrinking sheet in a hybrid nanofluid with a convective boundary condition." *International Journal of Numerical Methods for Heat & Fluid Flow* 29, no. 9 (2019): 3012-3038. <https://doi.org/10.1108/HFF-12-2018-0794>
- [40] Khan, Umair, Anum Shafiq, A. Zaib, and Dumitru Baleanu. "Hybrid nanofluid on mixed convective radiative flow from an irregular variably thick moving surface with convex and concave effects." *Case Studies in Thermal Engineering* 21 (2020): 100660. <https://doi.org/10.1016/j.csite.2020.100660>
- [41] Sreedevi, P., P. Sudarsana Reddy, and Ali Chamkha. "Heat and mass transfer analysis of unsteady hybrid nanofluid flow over a stretching sheet with thermal radiation." *SN Applied Sciences* 2, no. 7 (2020): 1-15. <https://doi.org/10.1007/s42452-020-3011-x>
- [42] Hayat, Tanzila, and S. Nadeem. "Heat transfer enhancement with Ag-CuO/water hybrid nanofluid." *Results in Physics* 7 (2017): 2317-2324. <https://doi.org/10.1016/j.rinp.2017.06.034>
- [43] Anuar, Nur Syazana, Norfifah Bachok, and Ioan Pop. "Radiative hybrid nanofluid flow past a rotating permeable stretching/shrinking sheet." *International Journal of Numerical Methods for Heat & Fluid Flow* 31, no. 3 (2020): 914-932. <https://doi.org/10.1108/HFF-03-2020-0149>
- [44] Dero, Sumera, Liaquat Ali Lund, Zahir Shah, Ebenezer Bonyah, and Wejdan Deebani. "Numerical Analysis of Hybrid Nanofluid of Streamwise and Cross Flow with Thermal Radiation Effect: Duality and Stability." *Mathematical Problems in Engineering* 2021 (2021).
- [45] Asghar, Adnan, Liaquat Ali Lund, Zahir Shah, Narcisa Vrinceanu, Wejdan Deebani, and Meshal Shutaywi. "Effect of Thermal Radiation on Three-Dimensional Magnetized Rotating Flow of a Hybrid Nanofluid." *Nanomaterials* 12, no. 9 (2022): 1566. <https://doi.org/10.3390/nano12091566>
- [46] Shoaib, Muhammad, Muhammad Asif Zahoor Raja, Muhammad Touseef Sabir, Saeed Islam, Zahir Shah, Poom Kumam, and Hussam Alrabaiah. "Numerical investigation for rotating flow of MHD hybrid nanofluid with thermal radiation over a stretching sheet." *Scientific Reports* 10, no. 1 (2020): 1-15. <https://doi.org/10.1038/s41598-020-75254-8>
- [47] Prasad, Ajay K., and Jeffrey R. Koseff. "Combined forced and natural convection heat transfer in a deep lid-driven cavity flow." *International Journal of Heat and Fluid Flow* 17, no. 5 (1996): 460-467. [https://doi.org/10.1016/0142-727X\(96\)00054-9](https://doi.org/10.1016/0142-727X(96)00054-9)
- [48] Waini, Iskandar, Anuar Ishak, and Ioan Pop. "Mixed convection flow over an exponentially stretching/shrinking vertical surface in a hybrid nanofluid." *Alexandria Engineering Journal* 59, no. 3 (2020): 1881-1891. <https://doi.org/10.1016/j.aej.2020.05.030>
- [49] Merkin, J. H. "Mixed convection boundary layer flow on a vertical surface in a saturated porous medium." *Journal of Engineering Mathematics* 14, no. 4 (1980): 301-313. <https://doi.org/10.1007/BF00052913>
- [50] Merkin, J. H. "On dual solutions occurring in mixed convection in a porous medium." *Journal of Engineering Mathematics* 20, no. 2 (1986): 171-179. <https://doi.org/10.1007/BF00042775>

- [51] Waini, Iskandar, Anuar Ishak, Teodor Groşan, and Ioan Pop. "Mixed convection of a hybrid nanofluid flow along a vertical surface embedded in a porous medium." *International Communications in Heat and Mass Transfer* 114 (2020): 104565. <https://doi.org/10.1016/j.icheatmasstransfer.2020.104565>
- [52] Waini, Iskandar, Anuar Ishak, and Ioan Pop. "Hybrid nanofluid flow towards a stagnation point on an exponentially stretching/shrinking vertical sheet with buoyancy effects." *International Journal of Numerical Methods for Heat & Fluid Flow* 31, no. 1 (2020): 216-235. <https://doi.org/10.1108/HFF-02-2020-0086>
- [53] Zainal, Nurul Amira, Roslinda Nazar, Kohilavani Naganthran, and Ioan Pop. "MHD mixed convection stagnation point flow of a hybrid nanofluid past a vertical flat plate with convective boundary condition." *Chinese Journal of Physics* 66 (2020): 630-644. <https://doi.org/10.1016/j.cjph.2020.03.022>
- [54] Khashi'ie, Najiyah Safwa, Norihan Md Arifin, Roslinda Nazar, Ezad Hafidz Hafidzuddin, Nadiyah Wahid, and Ioan Pop. "Magnetohydrodynamics (MHD) axisymmetric flow and heat transfer of a hybrid nanofluid past a radially permeable stretching/shrinking sheet with Joule heating." *Chinese Journal of Physics* 64 (2020): 251-263. <https://doi.org/10.1016/j.cjph.2019.11.008>
- [55] Yan, Liang, Sumera Dero, Ilyas Khan, Irshad Ali Mari, Dumitru Baleanu, Kottakkaran Sooppy Nisar, El-Sayed M. Sherif, and Hany S. Abdo. "Dual solutions and stability analysis of magnetized hybrid nanofluid with joule heating and multiple slip conditions." *Processes* 8, no. 3 (2020): 332. <https://doi.org/10.3390/pr8030332>
- [56] Jamil, Muhammad, and Najeeb Alam Khan. "Slip effects on fractional viscoelastic fluids." *International Journal of Differential Equations* 2011 (2011). <https://doi.org/10.1155/2011/193813>
- [57] Andersson, Helge I. "Slip flow past a stretching surface." *Acta Mechanica* 158, no. 1 (2002): 121-125. <https://doi.org/10.1007/BF01463174>
- [58] Hayat, Tanzila, S. Nadeem, and A. U. Khan. "Rotating flow of Ag-CuO/H<sub>2</sub>O hybrid nanofluid with radiation and partial slip boundary effects." *The European Physical Journal E* 41, no. 6 (2018): 1-9. <https://doi.org/10.1140/epje/i2018-11682-y>
- [59] Aly, Emad H., and I. Pop. "MHD flow and heat transfer near stagnation point over a stretching/shrinking surface with partial slip and viscous dissipation: Hybrid nanofluid versus nanofluid." *Powder Technology* 367 (2020): 192-205. <https://doi.org/10.1016/j.powtec.2020.03.030>
- [60] Zainal, Nurul Amira, Roslinda Nazar, Kohilavani Naganthran, and Ioan Pop. "Unsteady stagnation point flow of hybrid nanofluid past a convectively heated stretching/shrinking sheet with velocity slip." *Mathematics* 8, no. 10 (2020): 1649. <https://doi.org/10.3390/math8101649>
- [61] Tiwari, Raj Kamal, and Manab Kumar Das. "Heat transfer augmentation in a two-sided lid-driven differentially heated square cavity utilizing nanofluids." *International Journal of Heat and Mass Transfer* 50, no. 9-10 (2007): 2002-2018. <https://doi.org/10.1016/j.ijheatmasstransfer.2006.09.034>
- [62] Hale, N. P. "A sixth-order extension to the matlab bvp4c software of j. kierzenka and l. shampine." *Department of Mathematics, Imperial College London* (2006).
- [63] Lund, Liaquat Ali, Zurni Omar, and Ilyas Khan. "Quadruple solutions of mixed convection flow of magnetohydrodynamic nanofluid over exponentially vertical shrinking and stretching surfaces: Stability analysis." *Computer Methods and Programs in Biomedicine* 182 (2019): 105044. <https://doi.org/10.1016/j.cmpb.2019.105044>
- [64] Hafidzuddin, E. H., R. Nazar, N. M. Arifin, and I. Pop. "Boundary layer flow and heat transfer over a permeable exponentially stretching/shrinking sheet with generalized slip velocity." *Journal of Applied Fluid Mechanics* 9, no. 4 (2016): 2025-2036. <https://doi.org/10.18869/acadpub.jafm.68.235.24834>
- [65] Ghosh, Sudipta, and Swati Mukhopadhyay. "Stability analysis for model-based study of nanofluid flow over an exponentially shrinking permeable sheet in presence of slip." *Neural Computing and Applications* 32, no. 11 (2020): 7201-7211. <https://doi.org/10.1007/s00521-019-04221-w>